COMPUTATIONAL STUDIES ON ELASTOMERIC DIAPHRAGM OF MEMBRANE PUMP PERFORMANCE USING PURELY LAGRANGIAN AND COUPLED EULERIAN-LAGRANGIAN METHODS

MOHD NORSHAHID BIN MOHD IDRIS

RESEARCH REPORT SUBMITTED TO THE FACULTY OF ENGINEERING UNIVERSITY OF MALAYA, IN PARTIAL FULFILMENT OF THE REQUIREMENTS FOR THE DEGREE OF MASTER OF MECHANICAL ENGINEERING

2019

UNIVERSITY OF MALAYA

ORIGINAL LITERARY WORK DECLARATION

Name of Candidate: **Mohd Norshahid bin Mohd Idris**

Matric No: **KQK170003**

Name of Degree: **Master of Mechanical Engineering**

Title of Project Paper/Research Report/Dissertation/Thesis ("this Work"):

Computational studies on elastomeric diaphragm of membrane pump performance using purely Lagrangian and Coupled Eulerian-Lagrangian methods

Field of Study: **Mechanical Engineering – Solid & Fluids Mechanics**

I do solemnly and sincerely declare that:

(1) I am the sole author/writer of this Work;
(2) This Work is original;
(3) Any use of any work in which copyright exists was done by way of fair dealing and for permitted purposes and any excerpt or extract from, or reference to or reproduction of any copyright work has been disclosed expressly and sufficiently and the title of the Work and its authorship have been acknowledged in this Work;
(4) I do not have any actual knowledge nor do I ought reasonably to know that the making of this work constitutes an infringement of any copyright work;
(5) I hereby assign all and every rights in the copyright to this Work to the University of Malaya ("UM"), who henceforth shall be owner of the copyright in this Work and that any reproduction or use in any form or by any means whatsoever is prohibited without the written consent of UM having been first had and obtained;
(6) I am fully aware that if in the course of making this Work I have infringed any copyright whether intentionally or otherwise, I may be subject to legal action or any other action as may be determined by UM.

Candidate's Signature Date:

Subscribed and solemnly declared before,

Witness's Signature Date:

Name:

Designation:

ABSTRACT

This research project was conducted to explore the capabilities of Abaqus fluid-structural analysis using Coupled Eulerian-Lagrangian (CEL) elements in simulating fluid induced deformation on a diaphragm of commercially available air operated double diaphragm pump. Result of the CEL analyses are compared with fully Lagrangian element which in this study was run in dynamic explicit using Abaqus/Explicit solver for sake of consistency. Previous numerical studies of quasi-static analyses (Implicit) were found not able to simulate the fluid induced deformation on the diaphragm. An FKM based elastomer from Freudenberg-NOK Sealing Technologies which typically used in diaphragm application and material properties of water was chosen in this study. The CEL analyses were found to be able to simulate the deformation that was cause by the fluid flow. However, significant effort in terms of pre-processing (defeaturing the models) and trouble-shooting are required to obtain convergence on the CEL analysis. On the other hand, the fully Lagrangian analysis was easy to setup and very stable in terms of convergence. Without correlation study with the actual part, it is not known whether the FE simulation result is accurate. However, these results and observations are useful in determining the capabilities of the CEL method by Abaqus.

ABSTRAK

Projek penyelidikan ini telah dijalankan untuk meneroka keupayaan analisis struktur cecair Abaqus menggunakan elemen Eulerian-Lagrangian (CEL) dalam menganalisis perubahan bentuh diafragma yang di sebabkan oleh aliran bendalir di dalam 'air operated double diaphragm pump' (AODD). Keputusan analisis menggunakan CEL domain dibandingkan dengan domain Lagrangian sepenuhnya yang dalam kajian ini dijalankan secara dinamik explicit menggunakan Abaqus/Explicit solver untuk mendapatkan result yang konsisten. Kajian numerik yang lepas yang dijalankan menggunakan analisis kuasi statik (Implicit) di dapati tidak dapat meniru perubahan bentuk yang di sebabkan oleh aliran bendalir pada diafragma. Elastomer berasaskan FKM dari Freudenberg-NOK Sealing Technologies yang biasanya digunakan dalam aplikasi diafragma dan sifat bahan air dipilih dalam kajian ini. Analisis CEL didapati dapat mensimulasikan perubahan bentuk diafragma yang disebabkan oleh aliran bendalir. Walau bagaimanapun, usaha yang tinggi dari segi pra-pemprosesan (memudahkan model) dan penyelesaian masalah (trouble-shooting) diperlukan untuk mendapatkan penyelesaian pada analisis CEL. Sebaliknya, analisis Lagrangian sepenuhnya mudah untuk di sediakan dan sangat stabil dari segi pengiraan. Tanpa kajian korelasi dengan keadaan sebenar, tidak diketahui sama ada keputusan FE simulasi adalah tepat. Walau bagaimanapun, keputusan dan pemerhatian ini berguna dalam menentukan keupayaan kaedah CEL oleh Abaqus.

ACKNOWLEDGEMENTS

First and foremost I praise and acknowledge Allah, the most gracious and the most merciful, for giving me the strength and ability to complete this study.

My deepest gratitude goes to my supervisor Ir. Dr. Alex Ong Zhi Chao for his support and advice during this work.

Special thanks goes to Michel S. LeDuc Jr., Engineering Analysis Director of Global CAE for Freudenberg-NOK Sealing Technologies for his endless advice and for allowing the utilization of FNST owned software and hardware to complete this study.

Last but not least, I would like to express my sincerest appreciation to my families, especially my wife who has been very understanding thorough the entire length of this study.

TABLE OF CONTENTS

LIST OF FIGURES

LIST OF TABLES

LIST OF SYMBOLS AND ABBREVIATIONS

Symbols	Description
a	Acceleration
b	Body force
c_d	Dilatory wave speed
C_{ijk}	Material constant that describes shear behavior
D_i	Material constant that describe the compressibility
E	Total energy
F	Total force
I	Internal Load
I_1, I_2 & I_3	Strain invariants of the deviatoric strain
J_{el}	Elastic volume ratio
L_e	Minimum element length
M	Lumped Mass
N	Number of terms in the strain energy functions
p	Pressure
P	External Load
$\dot{Q}$	Rate of quantity of heat
t	Time
TPE	Thermoplastic elastomer
v	Flow velocity
Δt_{crit}	Stable time increment
$\dot{\varepsilon}$	Strain rate
ρ	Density
σ	Stress

Abbreviations	Description
2D	Two dimensional
3D	Three dimensional
ALE	Arbitrary Lagrangian-Eulerian
AODD	Air Operated Double Diaphragm
ASTM	American Society for Testing and Materials
CAD	Computer Aided Design
CEL	Coupled Eulerian-Lagrangian
CFD	Computational Fluid Dynamic
cpm	Cycles per minute
CSE	Co-Simulation Engine
DOF	Degree of freedom
EOS	Equation of state
EVF	Eulerian Volume Fraction
FEA	Finite Element Analysis
FEM	Finite Element Method
FKM	Fluoroelastomer
FSI	Fluid Structure Interaction
psi	pound per square inch
PTFE	Polytetrafluoroethylene
UT	Uniaxial tension

CHAPTER 1: INTRODUCTION

1.1 Background of the Problem

In general, a diaphragm is an engineered round sheet of semi-flexible or often highly-flexible materials that is secured at the inner and outer edges / inside and outside diameter. The diaphragms functions as a seal between two fluids chambers that will be actuated based on pressure differences between both contained fluids. The reciprocating actions of the diaphragm push and pull the fluids and acted as a pump without the need of lubrications. This type of pump is usually referred as diaphragm or membrane pump.

Typically, a membrane pump design will have compressed air (pneumatic) or hydraulic fluids on one side that is constantly varied in pressure and a transport fluid on the other side. The varied pressure causes the diaphragm to actuate which will cause fluctuations of volume that forces fluids out of the chamber and pulls more fluids in from its source.

The diaphragm of the membrane pump is typically made out of an elastomer, thermoplastic or Teflon. It also utilizes a suitable type of valves on either side of the diaphragm to aid in the pumping and prevents a reverse flow of the transport fluid.

1.2 Problem Statement

Current simulation method of quasi-static analysis using pure Lagrangian formulation to predict the performance of an elastomeric diaphragm could be an oversimplification of the problem. The current method predicts the maximum nominal strain and deformed shape of the diaphragm based on uniform pressure distributions

which will mechanically actuated the diaphragms. In actual situations, the properties (flow rate, viscosity, etc.) of the fluids will greatly govern the conditions of the elastomeric diaphragms. Hence, the pressure distributions on the diaphragms surfaces are most likely non-uniform.

1.3 Project Objectives

The objectives of this study are as follows:

- Develop an elastomeric diaphragm concept that is suitable for membrane pump based upon commercially available diaphragm pump.
- Evaluate the maximum nominal principal strain level and deformations of the developed elastomeric diaphragm concept using Coupled Eulerian-Lagrangian (CEL) analysis method.
- Compare the result from CEL method with purely Lagrangian method using uniform & fixed pressure surfaces of the compressed air and fluid.

1.4 Report Outline

The first chapter on this report highlights the background of the problems and the objectives of the research project. Further explanations of the problems are describes in chapter 2. Other than that, review of past related research, relevant information of finite element analysis and elastomer are outlined as well.

In chapter 3, the methodology that was used in this study is explained and the result of the finite element analyses are shown and discussed in chapter 4.

Finally, based on the observations and findings, conclusion and recommendation are drawn in chapter 5

CHAPTER 2: LITERATURE REVIEW

2.1 Diaphragm Pump

Diaphragm is a sheet of flexible material that acts as a seal between two chambers and will deform upwards or downwards depending on the pressure difference between those chambers (Freudenberg Simrit GmbH & Co. KG, 2007). There are three types of material that are usually use in diaphragms which are elastomer, thermoplastic elastomer (TPE) and Polytetrafluoroethylene (PTFE) (Jack, 2015).

Diaphragm pump or air operated double diaphragm (AODD) pump are designed to transport highly viscous or abrasive material using the diaphragm principles. This type of pump is known to be reliable and relatively easy to maintain due to the fact that simple diaphragm design is typically used. Other than that, it requires less energy to operate due to reduction of friction (Söderholm, 2008). In operation, the AODD pump will automatically adjust the pumping rate based upon the viscosity of the fluid. As the fluid viscosity increase, the pumping speed will reduce until it stops when it can no longer capable of moving the fluid. This can prevent damage to the pump (Rozee, 2016).

When dealing with abrasive material, the separation of abrasive fluid from pump's moving parts has eliminate some issues that are found in other pump technology. This has result in an increase in time between maintenance, longer operational time and lower leakage risk (Johnson, 2014).

Many industries utilize this type of pump such as oil & gas, food processing, chemical transfer and many more. It is a preferred pump technology for chemical

manufacturers due to its reliability and cost effectiveness (Wilden Pump & Engineering, LLC, 2018).

As shown in Figure 2.1, compressed air is used to exert pressure on the diaphragm and center shaft. The compressed air will switch direction between two sets of diaphragm or chamber. Both sets of diaphragm are connected by the center shaft which allows both to move in harmony during pump operation. The movement of diaphragm creates a strong pressure to move the fluid through the valve. As one diaphragm push the fluid out of one chamber, the other diaphragm will pull in fluid into the other chamber at the same time. These mechanisms create a continuously pounding of fluid out of the pump. Common types of valves that can be found on AODD pump are valve balls (as shown in Figure 2.1) and flap valve type (Bowan, 1997).

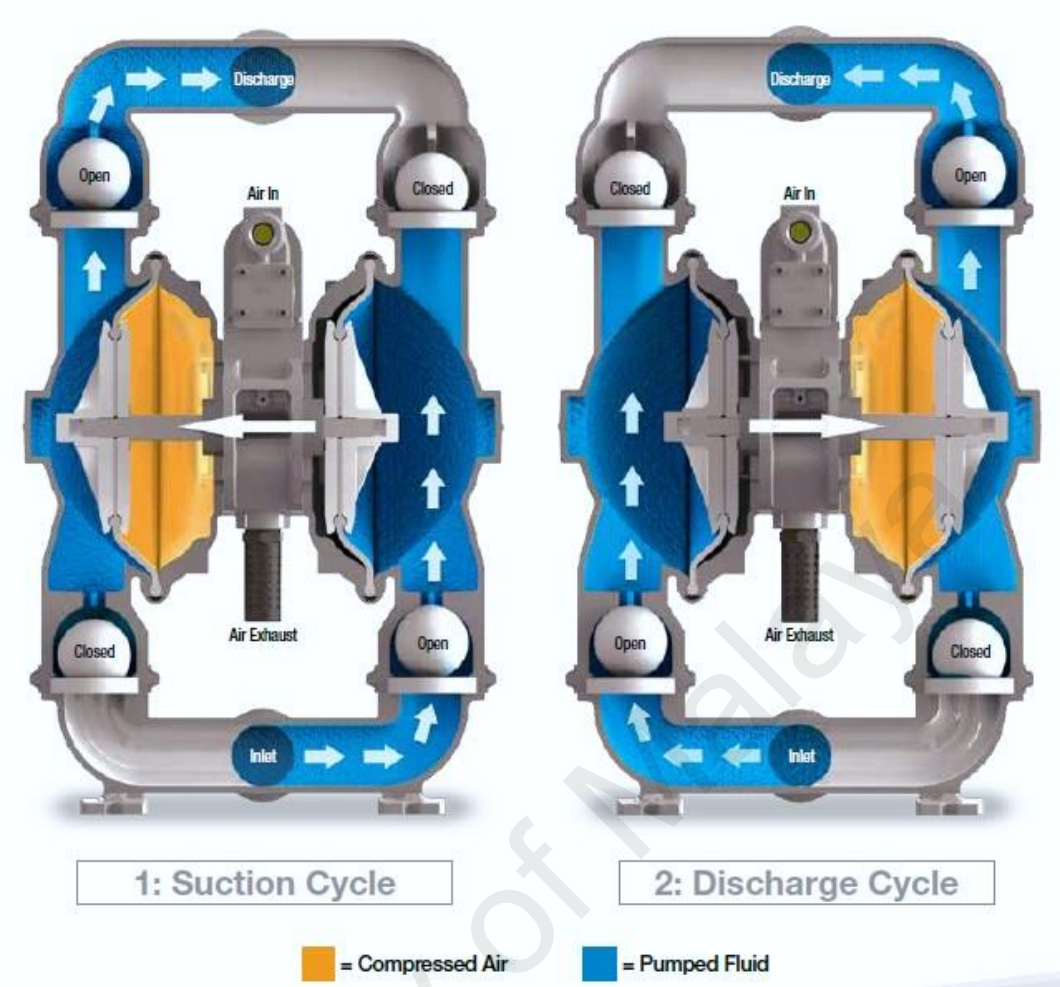

Figure 2.1: Operation of Air Operated Double Diaphragm Pump. Image taken from Standard Pump, Inc. (2013)

2.1.1 Common problems

The diaphragm main function in the membrane pump is not only to pump the fluid but also act as a layer that seal and separate the fluid from mixing with fluid in the other chamber. One of the common problems of membrane pump is cracking of the diaphragm (Mimmia & Pennacchi, 2001). This is usually due to fatigue failure because of high cyclic nature of the pump. Some pump manufacturers employs a double layer diaphragms design. The additional layer act as a safety seal when the main layer is rupture (Bubb & Freissler, 2010).

The other common problem in AODD pump is the loss of air at the end of pump stroke which is related to optimizing the technology related to the air distribution system (Brito & Jack, 2016).

In transferring extremely corrosive fluid, a diaphragm with good chemical resistance, high elasticity and low permeability to gases is important. Figure 2.2 shows the class of elastomer that can functions with respect to the service temperature and swelling in oil. This chart serve as a good tool for selecting class of elastomer that is capable in an application with that particular type of oil but it couldn't be used to predict the material's resistance to other type of fluid or chemical (Stahl, 2006). The resistance to chemical attack on the diaphragm can be improved by the use of PTFE and elastomer combination. However, the use of PTFE coating on an elastomeric diaphragm limits the amount of pump stroke which result in lower flow rate (Aerts & Gut, 2007). Freudenberg Simrit has added a fabric layer in the diaphragm which is found to improve its strength-bearing capabilities while maintaining resistance to chemical attack with PTFE layer on the other sides (Optimised diaphragm design, 2004). The additional layers bonded to elastomer will result in an increase in manufacturing effort. These layers should be bonded securely with elastomer or it could suffer premature failure (Warren & Smith, 2007).

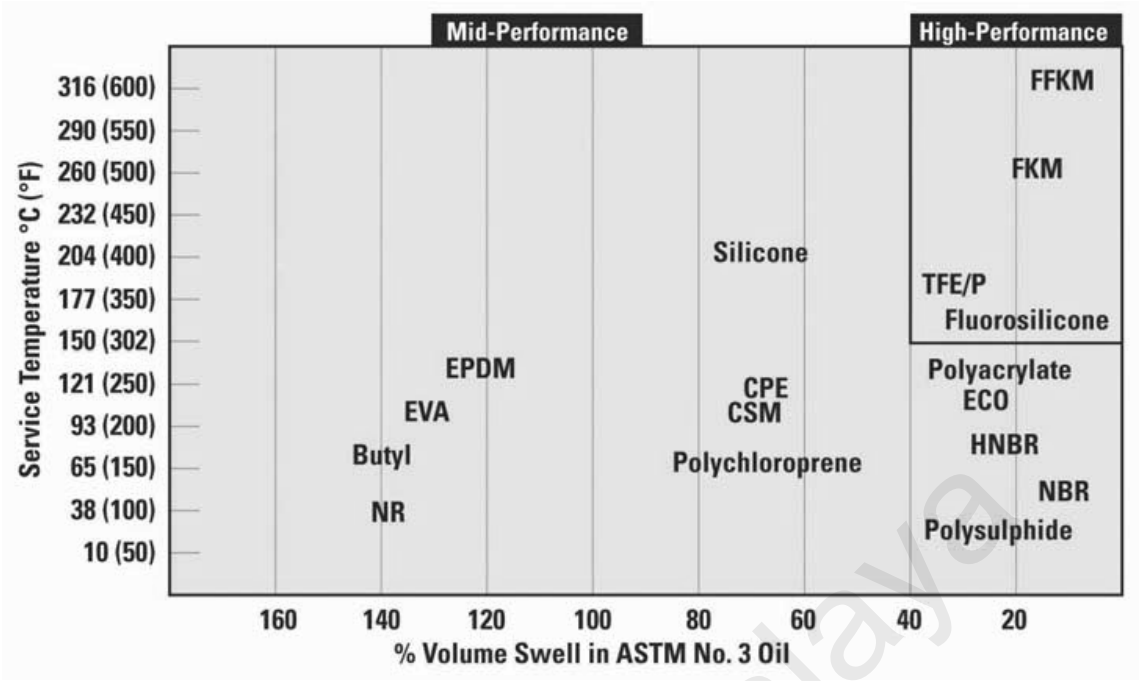

Figure 2.2: Types of elastomers with respect to its resistance to heat aging and swelling in ASTM No. 3 Oil based on SAE J200 (ASTM D2000). Image taken from Stahl (2006)

2.1.2 Review of FEA in analyzing diaphragm deformation

There are very limited academic literatures on diaphragm deformation analysis using finite element method (van Rijswick, 2017). Prior to work by van Rijswick (2017), the only known academic research on pump diaphragm have been done at Erlangen University in Germany in the 80's and 90's. Work done by Georgiadis (1988) was an experimental and numerical studies on metal diaphragm stresses and then Völkl (1992) was focussing on the clamping effect of the metal diaphragm. Furthermore, experimental and numerical study by Schlücker (1993) was performed on a PTFE diaphragm. All numerical study done by Erlangen University was a quasi-static analysis with fixed defined pressure surfaces on a two dimensional (2D) axisymmetric and 3D shell model. These studies weren't able to simulate the local buckling or snap-through effect of the diaphragm due to numerical instability.

The latest numerical studies (and experimental) on elastomeric diaphragm was performed by van Rijswick (2017) using three Dimensional (3D) shell diaphragm as quasi-static analysis and also with Fluid-Structural Interaction (FSI) approach. He found that quasi-static structural analysis is not sufficient to predict failure on the elastomeric diaphragm due to the absent of the effect of fluid momentum and turbulance inside the pump chamber. However, his attempt with 3D shell diaphragm using FSI approached wasn't exactly correlate with the experimental result in terms of higher order deformations modes. Interestingly, his attempt using quasi-static analysis with hydrostatic pressure differences were able to correlate with the experiment in terms of snap-through behavior especially at the middle of stroke (discharge or suction).

2.2 Finite Element Analysis

The use of finite element method (FEM) can be seen started in the early 1900s. Richard Courant was widely considered as the first person who successfully developed the finite element method using piecewise polynomial interpolation over triangular element to investigate a torsion problem (Moaveni, 2015). Nowadays, FEM has been widely used to solve different kind of engineering problems. Some of the engineering problems that can be solve with FEM are structural (static stress, dynamic, etc.), heat transfer, electromagnetic, fluid flow, acoustics, and many more.

The basic steps in solving problem using FEM are pre-processing, calculation by solver and post-processing. In pre-processing, the model is discretized (meshed) into finite number of elements. Each element will contain certain number of nodes which are usually the integration point. The meshed element will assume a shape function to represent the physical behavior of the element and an equation for each element will be developed. Finally, the equations for all the elements are assembled into global stiffness

matrix to represent the entire problem. By applying material properties, initial condition, boundary conditions and loads, the solver will calculate and solve the global stiffness matrix to acquire result at the integration points such as displacement (static) or temperature (heat transfer). The calculated result will then be used to obtain other useful information in post-processing stage. Examples of useful result are principal stresses, strain, heat fluxes, etc.

There are a number of commercially available software for solving finite element analysis such as Abaqus, ANSYS, Altair HyperWorks, COMSOL Multiphysics, Nastra, LS-DYNA, and many more. These software are widely used in the industries and academics due to its ease of use, robustness and capabilities. With the advancement in computer technology, these software can be installed in a desktop computer which makes the cost of ownership relatively low. The commercial software also has the advantage of good customer support and latest updates.

2.2.1 Abaqus

Abaqus is a software suite for finite element analysis which was originally released in 1978 by Dr. David Hibbitt, Dr. Bengt Karlsson, and Dr. Paul Sorensen with the original name Hibbitt, Karlsson & Sorensen, Inc., (HKS). The name Abaqus is used after the original company (HKS) was acquired by Dassault Systèmes in 2005.

The main solver modules in Abaqus are Abaqus/Standard and Abaqus/Explicit (Simulia, 2006) as shown in Figure 2.3. Abaqus/Standard is a general purpose finite element module which is highly capable of analyzing numerous types of problems (static, dynamic, non-structural, etc.). The Abaqus/Explicit is an explicit dynamic finite element module. The comparison between Abaqus/Standard and Abaqus/Explicit are explained in Table 2.1.

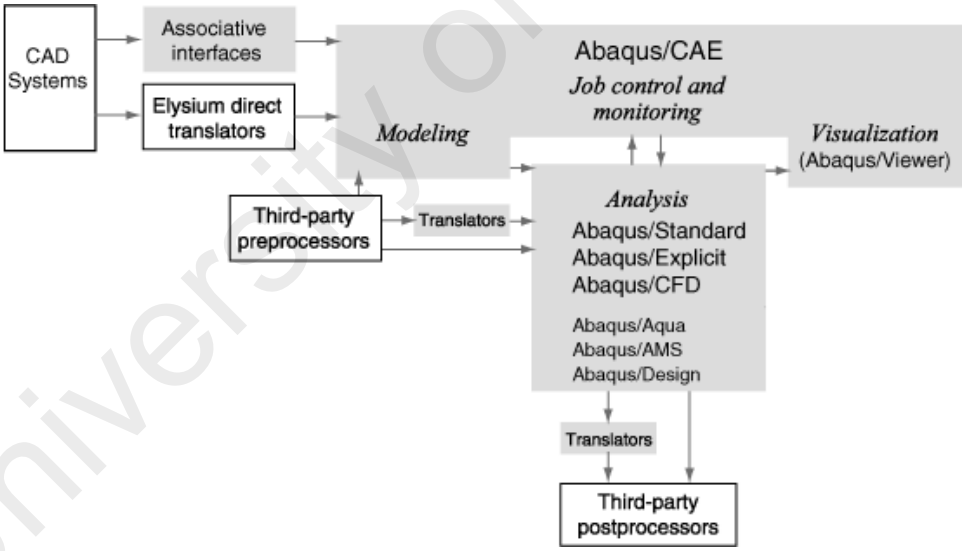

Figure 2.3: Suite of FEA modules from Abaqus. Image taken from Simulia (2006)

Table 2.1:Comparison between Abaqus/Standard & Abaqus/Explicit. Taken from Simulia (2015a)

Criteria	Abaqus/Standard	Abaqus/Explicit
Capabilities	• Linear & non-linear static • Linear dynamic • Low speed nonlinear dynamic • Nonlinear heat transfer • Coupled temperature-displacement (quasi-static) • Coupled thermal-electrical • Mass diffusion problem • Structural acoustics	• High speed dynamics (short durations) • Large, non-linear, quasi-static analysis • Highly discontinuous post-buckling and collapse simulation • Extreme deformations • Coupled temperature-displacement (dynamic) • Structural acoustics
Unknown values	Unknown values are obtain from current information (current time)	Unknown value obtain from already known information
Iteration / convergence criteria	Iterative and convergence checking are required	no iteration and convergence checking required
Time increment	Need to maintain force equilibrium which sometimes requires much iteration. Once convergence is achieved, time increment can be very large	time increment has to be very small but large number of increments can be calculated efficiently
Computational time	Based on numbers of degrees of freedom (DOF) and iterations count	Based on number of elements, stable time increment and duration of the step

2.2.2 Abaqus/Explicit Solver

The Abaqus/Explicit is a dynamic explicit solver by Abaqus. It will solve the general dynamic equilibrium equation as shown in Equation (2.1)

$$F = Ma \tag{2.1}$$

where F is total forces, M is lumped mass and a is acceleration. Explicit dynamic is a mathematical technique for integrating the equations of motions through time. The integration method used by Abaqus is forward Euler or central difference algorithms. This means that the unknown values are obtained from already known information. By utilizing the explicit integration algorithms, the lumped mass matrix, M is calculated in the global mass matrix as shown in Equation (2.2)

$$a = M^{-1}.F = M^{-1}.(P - I) \tag{2.2}$$

where P is the external load and I is the internal load. The calculation will provide us with nodal accelerations at any given time.

The explicit solver is known to be conditionally stable. A stable time increment Δt_{crit} has to be determined in order to have a conditionally stable solution. The stable time increment uses by Abaqus/Explicit is shown in Equation (2.3)

$$\Delta t_{crit} = \frac{L_e}{c_d} \tag{2.3}$$

where L_e is the minimum element length and c_d is the dilatory wave speed (Simulia, 2016). As no convergence criteria exist, it is difficult to control the solution.

2.2.3 Mesh domains

There are three types of relationships between the meshes and the underlying material that are provided by Abaqus/Explicit which are:

1. Lagrangian
2. Eulerian
3. Arbitrary Lagrangian-Eulerian (ALE)

In Lagrangian domain, elements and nodes are fixed within the material. It is easy to track free surfaces and apply boundary conditions but the meshes will be highly distorted under high strain.

In Eulerian domain, the elements and nodes stay fixed but the material (and its motion / deformation) moves through the fixed meshes. This type of domain is suitable for application that requires extreme deformation, up to and including fluid flow. The implementation of Eulerian domain in Abaqus/Explicit is via volume of fluid in each element. Initially all Eulerian elements are empty (void) by default and it is filled by material using volume fraction. As the analysis progresses, the material inside the Eulerian domain is tracked in Abaqus using Eulerian Volume Fraction (EVF) (Simulia, 2016). The void elements in the analysis didn't contain any mass or stiffness.

Lastly, in ALE domain or commonly refer as adaptive meshing, the mesh motion is constrained with other material motion at the boundaries. It is an adaptive meshing technique that combines the feature of Lagrangian and Eulerian analysis. With ALE, high quality meshes can be maintain throughout the analysis as the meshes are allow to move independently of the material. ALE is different than Eulerian as all the element is completely filled without any void with only single material within each element. The remapping of meshes or adaptive meshing in ALE is capable of limiting mesh distortion

in a simulation with large deformation which will definitely improve the accuracy and reliability of the result (Bakroon, Daryaei, Aubram, & Rackwitz, 2017).

2.2.4 Coupled Eulerian-Lagrangian (CEL)

The coupled Eulerian-Lagrangian (CEL) implementation in Abaqus is available in dynamic explicit solver. The fundamental equation that govern the motion of rigid and deformable bodies in CEL analysis are consist of conservation of mass (continuity), momentum (motion) and energy as describe in Equation (2.4), Equation (2.5), Equation (2.6) & Equation (2.7) as follows:

Conservation of mass (continuity):

$$\frac{D\rho}{Dt} + \rho\nabla \cdot v = \frac{\delta\rho}{\delta t} + v \cdot \nabla\rho + \rho\nabla \cdot v = 0 \tag{2.4}$$

Conservation of momentum (motion):

$$\rho\frac{Dv}{Dt} = \nabla \cdot \sigma + \rho b \tag{2.5}$$

$$\frac{Dv}{Dt} = \frac{\delta v}{\delta t} + \mathrm{v} \cdot \nabla\mathrm{v} \tag{2.6}$$

Conservation of energy:

$$\rho\frac{DE}{Dt} = \sigma \cdot \dot{\varepsilon} + \rho\dot{Q} \tag{2.7}$$

where $\frac{D()}{Dt}$ is total derivative, $\frac{\delta()}{\delta t}$ is partial derivative, ρ is density, t is time, ∇ is divergence, v is flow velocity, b is body force, E is total energy, σ is stress; $\dot{\varepsilon}$ is strain rate and $\dot{Q}$ is rate of quantity of heat.

Abaqus/Explicit always solves these equations and the notion of a material (solid or fluid) is introduce when specific constitutive assumptions are made. The chosen constitutive assumption for either a solid or fluid material will simplified the equations of motion appropriately such as into compressible Navier-Stokes equation, Euler equations, etc.

Sillem (2008) found that at each increment, Abaqus will remesh the Eulerian element (volume fraction) based on deformation of the Lagrange domain which explain the long computational time needed. On top of that, the he also found that the displacement of the fluid is calculated instead of velocity with no possibility of turbulence flow modeling. The Eulerian elements in CEL can be modeled as viscous compressible Newtonian fluid as shown in Equation (2.8)

$$\sigma = -p + 2\eta\dot{\varepsilon} \tag{2.8}$$

where σ is Cauchy stress tensor, p is pressure, η is the shear viscosity and $\dot{\varepsilon}$ is strain rate. The fluid (Eulerian) and structural (Lagrangian) contact interaction is calculated with general contact algorithm in Abaqus/Explicit.

The Abaqus CEL technique is found to not only able to predict movement of fluid inside a chamber but also the stresses, strains, displacement and other structural related output that is induced by the fluids movement (Li, Ding, & Sibal, 2010). Moreover, Qiu, Henke, & Grabe (2009) found that the CEL technique is capable of simulating complex problem that exhibit large deformation without encountering issue with severe element distortion which is a typical problem in fully Lagrangian meshes. Xiaoying, Jian, & Chunlong (2016) found that the CEL method is accurate in simulating contained fluids but suffer from high computational time especially with complex simulation configuration. They also found that the analyses are often non-converging due to

intrinsic algorithm. Other than that, Ducobu, et al (2017) found that the CEL formulation is also suitable in modeling metal cutting while Chmelnizkij, Nagula, & Grabe (2017) establish that the CEL analysis is able to simulate the densification of loose dry sand that is imparted by horizontal vibrations.

However, the Abaqus CEL technique is only suitable for fluid flow with low Reynolds number flow or laminar flow (Simulia, 2015b). Simulia Co-Simulation Engine (CSE) technology which allows a coupling of Computational Fluid Dynamic (CFD) codes with structural FEA codes is a more robust alternative in solving complex fluid flow (Blades, Luke, Kurkchubashe, Collins, & Miskovish, 2010). Other than that, work by Nieminen (2015) demonstrated the ability to simulate two-way FSI co-simulation between ANSYS Fluent CFD codes and Abaqus structural FEA by utilizing MpCCI (independent interface for coupling different simulation codes).

2.3 Elastomer

Elastomer is a term that is a derived from the words ‘elastic’ and ‘polymer’ as it is a polymer that can be elastically stretchable (substantially) and almost return back to its original shape when force is release. Elastomer is mostly thermoset but some is thermoplastic elastomer (TPE) (i.e. Santoprene™, Fluoreprene™, etc). There are many types of elastomer and most of them are rubber. Therefore, the term elastomer and rubber are usually used interchangeably.

The molecular structure of a vulcanized elastomer is often imagined as a ‘spaghetti and meatball’ structures. The ‘meatball’ is representing the cross-linking of the ‘spaghetti’ or known as chains. The cross linking of the chains occurs via a chemical reaction with the introduction of heat and other material such as Sulphur. This is also

known as vulcanization. The high elasticity of elastomer is obtain thru the ability of the chains to reconfigure themselves when stretches. The cross-linkages bonds ensure that the stretched elastomer is able to return to its initial shape when loads are removed.

2.3.1 Material Model

An elastomeric material is usually considered as material that undergoes large deformation (hyperelastic) under external loads without considerable permanent deformations after removing the load (Brinson & Brinson, 2015). Therefore, the stress-strain behavior of an elastomer is highly non-linear and a simple modulus of elasticity is insufficient.

The foundation of the phenomenological theory of rubber elasticity was first introduced by Ronald Rivlin (Rivlin, 1956). The strain energy density function, W that can be written as

$$W = Deviatoric\ term + Volumetric\ term \tag{2.9}$$

$$W = \sum_{i+j+k=1}^{n} C_{ijk}(I_1 - 3)^i (I_2 - 3)^j (I_3 - 1)^k + \sum_{i=1}^{n} \frac{1}{D_i}(J_{el} - 1)^{2i} \tag{2.10}$$

where I_1, I_2 & I_3 are the strain invariants of the deviatoric strain, C_{ijk} is material constant that describes shear behavior, J_{el} is elastic volume ratio, N is number of terms in the strain energy functions (must be positive) and $D_{i\ is}$ material constant that describe the compressibility

Strain energy function is an energy stored in material per unit volume (initial condition) as a function of strain at that point in material. The deviatoric term in strain energy function is representing the function of how the material's shape will behave or

deformed and the volumetric term (hydrostatic) is representing how the volume is changing under stress.

Assuming that elastomer is a nearly incompressible material, I_3 will always equal to 1. This is because the third invariant is the square of the volume ratio and it will remain constant if it is incompressible. This assumption simplify the terms in strain energy density function or polynomial model into Equation (2.11)

$$W = \sum_{i+j=1}^{n} C_{ij}(I_1 - 3)^i (I_2 - 3)^j + \sum_{i=1}^{n} \frac{1}{D_i}(J_{el} - 1)^{2i} \tag{2.11}$$

There are a numbers of hyperelastic material models that are available in Abaqus such as Mooney-Rivlin, Neo-Hookean, Yeoh, Ogden, Arruda-Boyce, Marlow, Van Der Waals etc. Each of them defines the strain energy function differently (Simulia, 2016). An experimental test data will be fit into appropriate material model or strain energy function that will represent the material's stress-strain behavior. As an example, neo-Hookean model is suitable for small strain (missing upturn at the end), Mooney-Rivlin model for moderate strain and Ogden for large strain (Ali, Hosseini, & Sahari, 2010).

In this study, Neo-Hookean material model was chosen with strain energy function, $W = C_{10}(I_1 - 3) + D_1(J - 1)^2$. The material coefficient, C_{10} and D_1 can be calculated either manually or using Abaqus/CAE pre-processor by feeding in the stress-strain data from uniaxial tension (UT) test.

2.3.2 Failure Criteria for Elastomer

In quasi-static FE analysis, the nodal deformation (and strain) in a structure is the actual measurement calculated as a result of external loading or displacement. Stress output is then calculated based upon the material modulus of elasticity and true strain. Both stress and strain have been used in FEA to predict performance or potential failure.

Any commercially available FE codes can output both stress and strain. However, only true stress is available as an output. Unlike stiff metal or plastic, highly strained elastomer will see significant change in its cross-sectional area. Therefore, it is inaccurate to use true stress output from FEA and compare with the UT test data to evaluate part performance. Note that it is standard practice to collect nominal stress and strain data from uniaxial tension test. Therefore, in order to use true stress as a failure criterion, sets of true stress and strain data are needed from the UT test which is not readily available most of the times.

As for using strain as failure criteria, the nominal strain is readily available as an FEA output which makes it easy and convenient to compare with the UT test result. The maximum principal nominal strain has been a primary indication for failure criteria used by Freudenberg-NOK Sealing Technologies as it focusses the evaluation on the highest tensile strain in the component (LeDuc Jr. M. S., 2003).

CHAPTER 3: METHODOLOGY

3.1 Introduction

This chapter explains the steps, assumption, method that was used to develop the FEA model of the diaphragm pump. In the beginning, how Computer Aided Design (CAD) of the diaphragm pump was developed is explained. Then, all relevant FEA parameters are discussed which includes the modeling assumptions, boundary condition, loads, material model, meshing, contacts and solver.

Two types of FEA were created in this study which is Coupled Eulerian-Lagrangian and fully Lagrangian model. Both models are solved using dynamic explicit solver from Abaqus.

3.2 CAD model of membrane pump

The Graco Husky 515 air operated double diaphragm (AODD) pump was chosen for this study. This particular pump was chosen because of availability of operating condition data and CAD model on their official website as shown in Figure 3.1. On top of that, the chosen pump is also the smallest pump that is made by Graco. The small pump size allow for reduce number of meshes required in the FE analysis. Some defeaturings was done to the downloaded CAD model to aid with the analysis setup and convergence.

The comparison between the as is and the simplified CAD model is shown in Figure 3.2. Only three of the pump components will be included in the FEA model. The inlet and outlet of the fluid chamber has been rotated to ease the meshing of the Eulerian

element. This will affect the fluid flow and diaphragm deformation but was necessary to aid with convergence and instability of the solver with contact between Eulerian and Lagrangian domain. This issue can be eliminated with the use of finer meshes of the Eulerian domain but was not possible in this study due to limited resources.

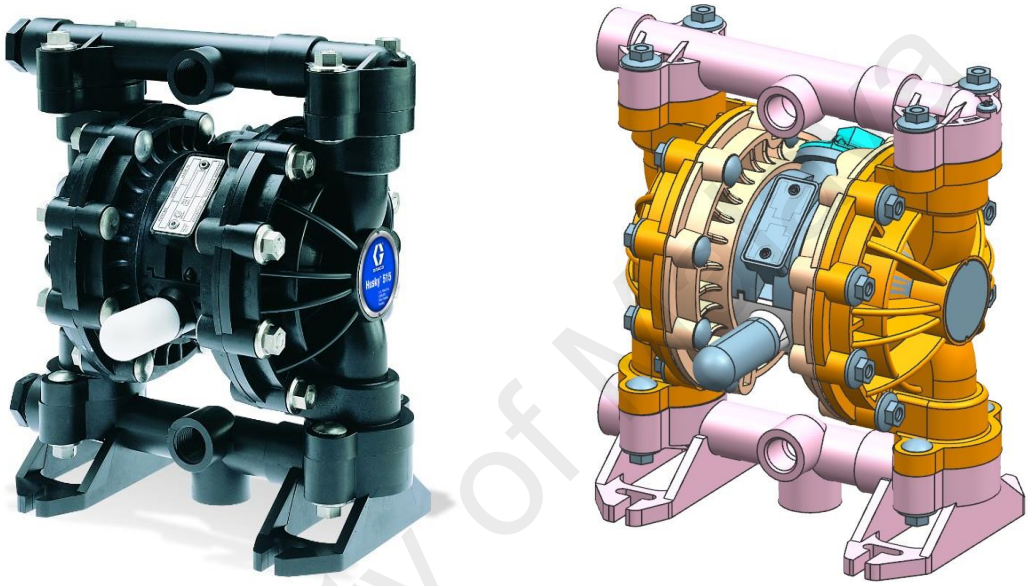

Figure 3.1: Husky 515 air operated diaphragm pump (actual and CAD model). Image taken from Graco Inc (2018)

The beads on the inner and outer diameter of the diaphragm are removed. As this change is predicted to not affecting how the convoluted diaphragm will deform, this simplification eliminates the need to resolve the initial over closure (limitation of Abaqus/Explicit) and expected issue with distorted elements of the compressed beads which will result in increase of computational time. The diaphragm of the downloaded CAD model is assumed to be as-molded geometry and it is positioned in the middle of the stroke (either suction or discharge).

The diaphragm in an actual pump is attached to the shaft with clamping discs. These clamping discs are modeled as single part in his study. As recommended by Abaqus,

generous radii are applied to the models to help with convergence of the analysis and reduce the possibilities of penetration of the Eulerian elements into Lagrangian domain. Further defeaturings was performed to the bottom chamber (compressed air chamber) by elimination all ribs which will allow the use of analytical rigid in the FEA model. This can potentially help to reduce the computational efforts especially when dealing with contacts. Inlet and outlet valve balls are not modeled to simplify the fluid flow. As found by Alberto, Manuel, & Andrés (2019), the fluid flow around the valve balls are very complex with issue with leakage and ball tapping. Due to limited resources, a simpler approach of using boundary condition has been chosen to model the valve.

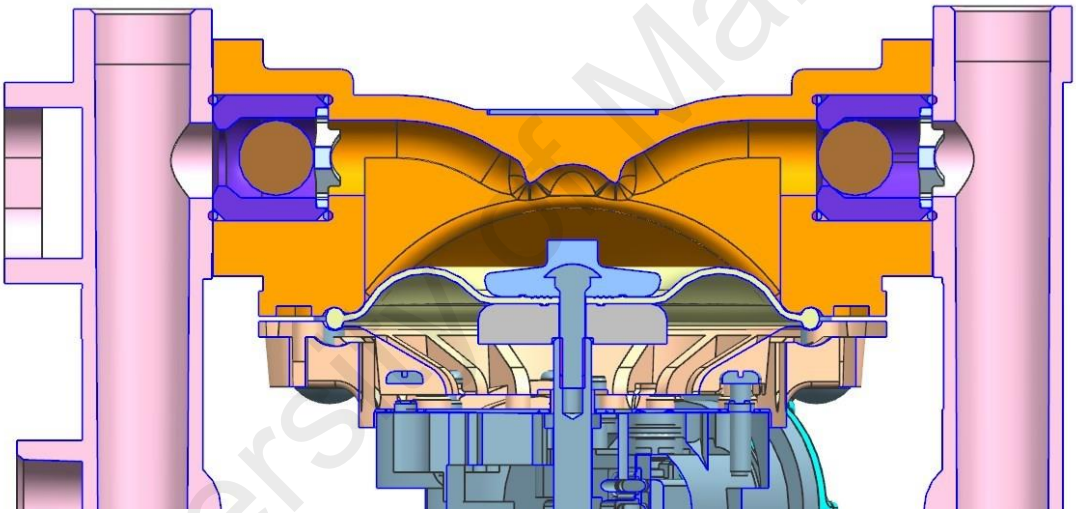

(a)

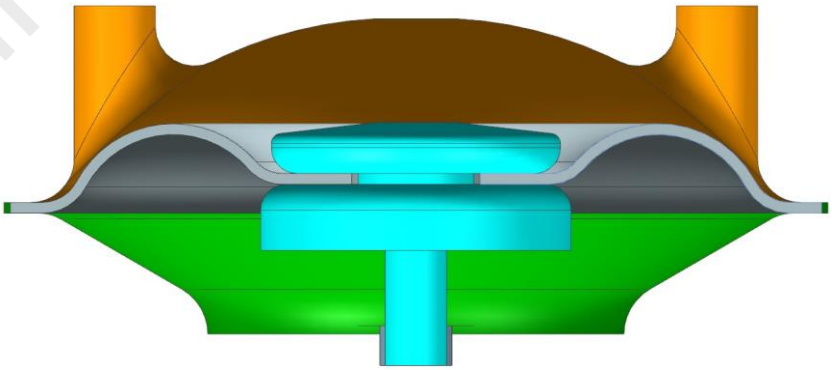

(b)

Figure 3.2: Comparison between cross-section of (a) ‘as is’ CAD model and (b) defeatured CAD model

3.3 Finite Element Analysis Setup

The elastomeric diaphragm is modeled as 180° deformable body in Lagrangian domain and the fluid is modeled as Eulerian element. All relevant pump components that will have contact interaction with fluid are modeled as discrete rigid and pump component that will not have contact with fluid is modeled as analytical rigid as shown in Figure 3.3.

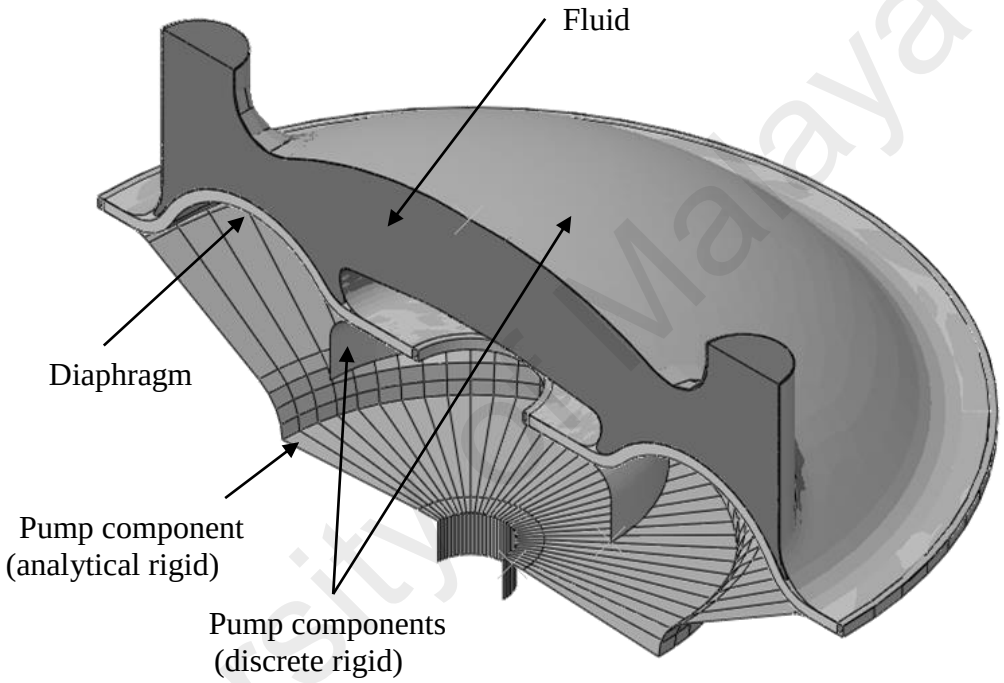

Figure 3.3: The 180° model of elastomeric diaphragm, fluid and pump components

3.3.1 Boundary Conditions & Loadings

As the beads on the diaphragm are removed, both inner and outer diameter of the diaphragm is fixed in the radial directions. The inlet and outlet of the fluids are constrained with velocity boundary condition as recommended by Abaqus. All other parts of the Eulerian elements are considered to flow freely which is the default setting. This means that the material will flows freely into and out of the mesh and any fluid parameters (pressure or velocity) will be gone once it gets out of the Eulerian meshes.

Compressed air pressure of 0.1MPa (14.5 psi) were chosen in the CEL model. Note that the chosen pressure magnitude is lower than the specification listed by the manufacturer which is between 30psi to 100psi. However, the reduced pressure is needed to reduce the diaphragm speed of deformation in the analysis which will potentially help with convergence. As for fully Lagrangian model, a pressure difference of 0.005MPa on fixed surfaces was applied either to compressed air or fluid side of the diaphragm depending on the pump stroke. All pressure was applied by linearly ramp up or down the pressure magnitude during each stroke (either discharge or suction).

3.3.2 Material - Elastomer

One of the typical material for diaphragm use by Freudenberg-NOK Sealing Technologies was chosen which is a fluoroelastomer (FKM) based elastomer. A uniaxial tension (UT) test was performed to the sample material according to proprietary test method that is modified from ASTM D412. This modified test method was developed to target appropriate strain based on determined preconditioning and relaxation to provide an improved steady-state stiffness response. The modified test method is based upon test method that was first suggested by James, Green & Simpson (1975) and further suggested by Yeoh (1990). In this study, Neo-Hookean material model is chosen because it is well known to be a stable material model. On top of that, the strain from the analysis is expected to be relatively low. With expected convergence difficulty in CEL analysis, a stable material model may ease the trouble-shooting effort.

The stress-strain curve of Neo-Hookean material model is overlaid on top of the raw test data as shown in Figure 3.4. The chosen material model is considered acceptable up to 150% strain. The density of 1.25×10^{-9} Mg/mm^3 and Neo-Hookean coefficient of C_{10}=0.2912 MPa and D_1=0.0015 was used in this study.

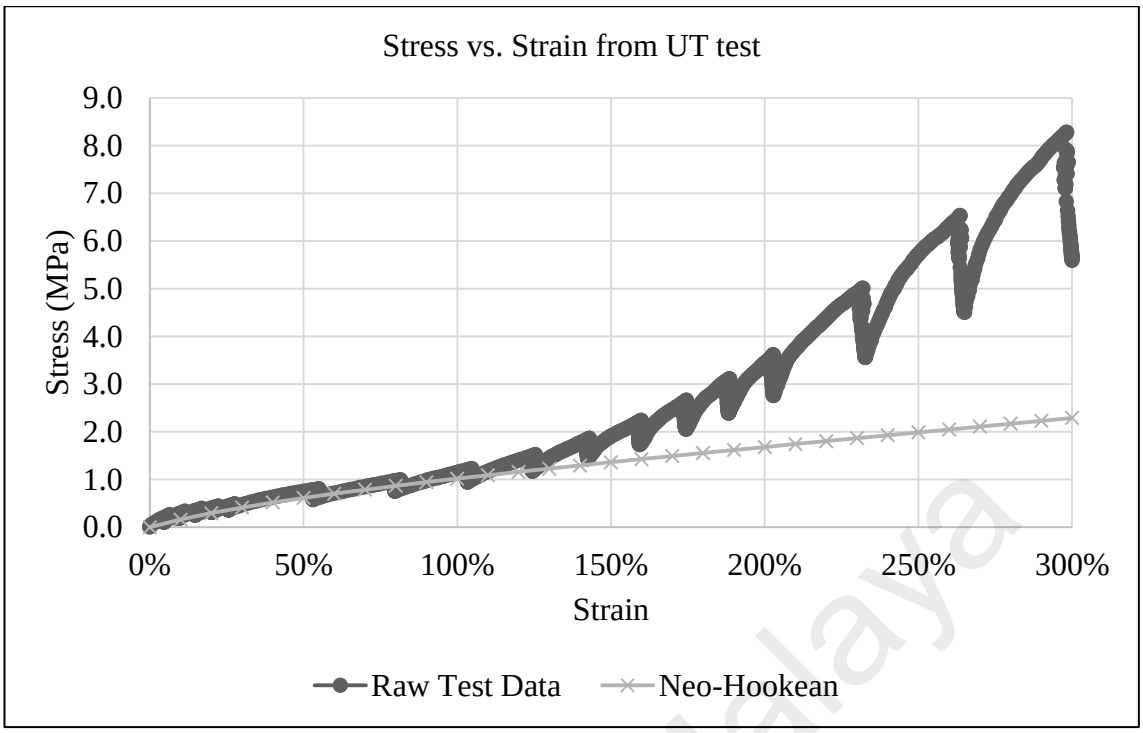

Figure 3.4: Material behavior of the chosen FKM material

3.3.3 Material - Fluid

The chosen diaphragm pump in this study is capable of transporting wide range of fluid types such as antifreeze, detergents, resins, polymers, motor oils, gear oils, hydraulic fluid, automatic transmission fluid, waste water and many more. Properties of water have been chosen for this study due to ease of gathering the required material properties.

The fluid in CEL analysis is modeled using equation-of-state (EOS). On top of that, the fluid wave speed (speed of sound) and viscosity are also needed. The EOS will provide hydrodynamic material model in which the material's volumetric strength is determined. This material model can be used to model a material that is assumed to not have any shear strength and only exhibit volumetric strength.

The density of 1.0×10^{-9} Mg/mm^3, viscosity from 1 mPa.s to 100,000 mPa.s and coefficient of EOS, $c_0 = 1.483 \times 10^6$ mm/s was used in this study.

3.3.4 Mesh

Both Lagrangian and Eulerian element were meshed with 8-node linear hexahedral elements (C3D8R & EC3D8R respectively). Abaqus/Explicit analysis requires the use of reduce integration elements with default hourglass control. This means that each element will contain only single integration point which is located in the middle of the element. The Eulerian elements are initially filled with void material by default. Volume fraction option is use to create material within the Eulerian elements.

As recommend by Abaqus, the Eulerian mesh must be fine enough to resolve details of the geometries or the solutions. The Eulerian mesh resolutions must be 3 to 5 elements of the smallest Lagrange domain. In this study, as local refinement is not possible, the Lagrange model must be coarse enough when compared with Eulerian meshes. Therefore, 2mm global seed was chosen for the diaphragm with 32 elements along the circumference as shown in Figure 3.5(a). A finer mesh for the Eulerian was created with 1mm global seed and 64 elements along the circumference as shown in Figure 3.5(b). Total elements for the diaphragm and fluid are 1920 and 178801 respectively. These mesh densities were chosen after numerous attempt to find the right balance between convergence, accuracies and computational time. With limited resources and various analyses to calculate, a finer mesh is not a feasible option. Figure 3.5 shows meshes of Lagrangian and Eulerian elements as described earlier.

A finer diaphragm meshes were created as show in Figure 3.6 with 106 elements along the circumference. The finer meshes will be used in fully Lagrangian dynamic explicit analysis and for comparison with the coarser meshes.

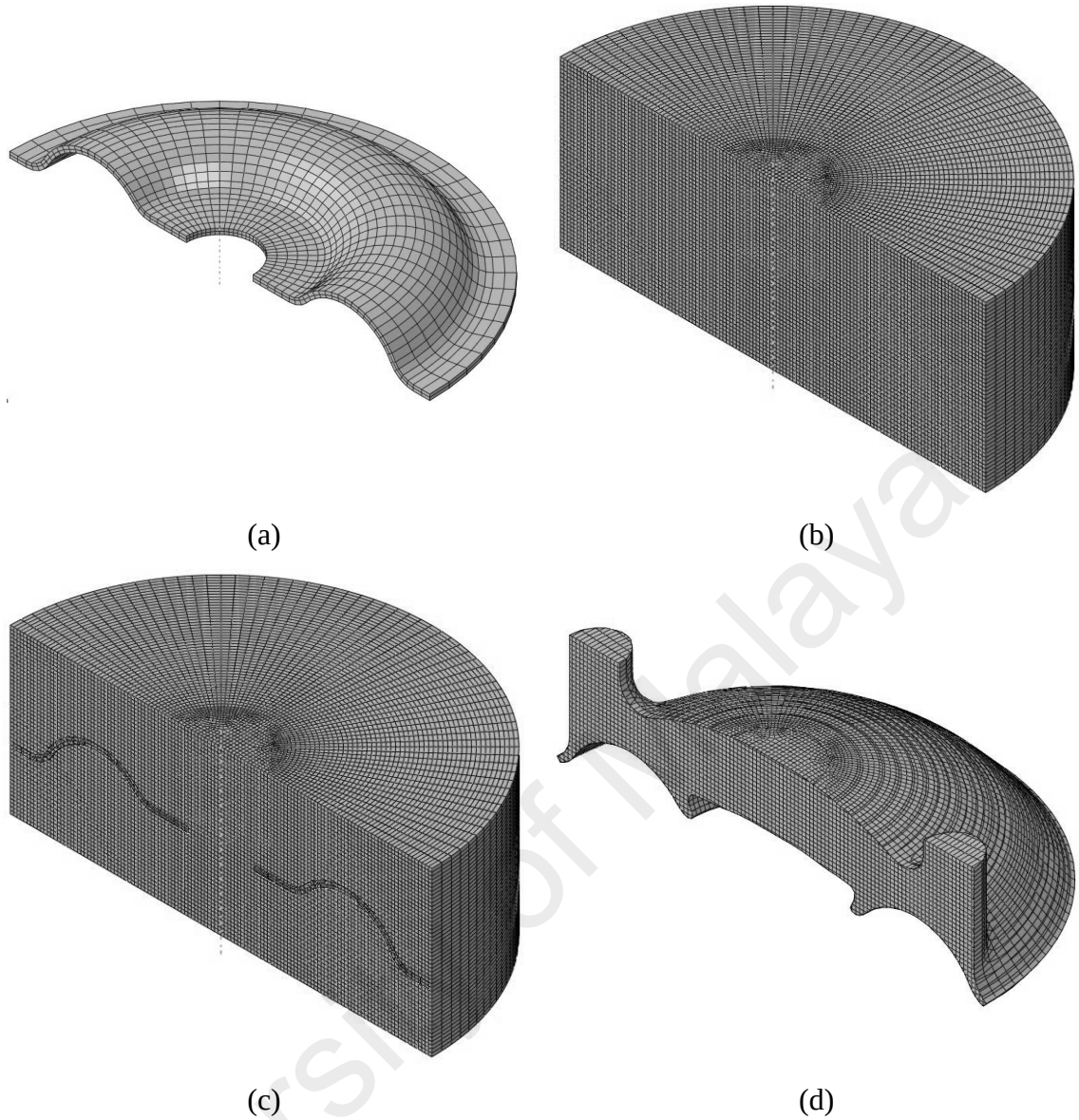

(a) (b)

(c) (d)

Figure 3.5: Meshes of (a) Lagrangian (diaphragm), (b) Eulerian (fluid), (c) overlaid of Lagrangian and Eulerian elements and (d) Eulerian element with volume fraction

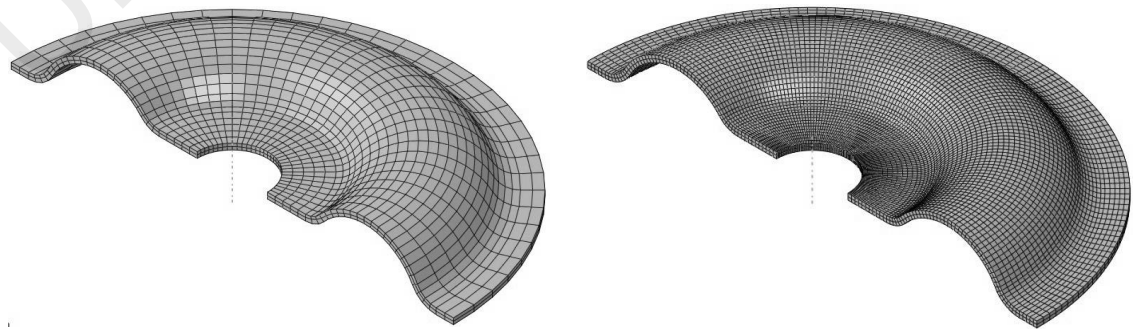

(a) (b)

Figure 3.6: Diaphragm meshes with (a) 32 and (b) 106 elements along the circumference.

3.3.5 Contact Interaction

To define the contact interaction in the analyses, general contact algorithm was used in this study. Friction coefficient of 0.1 was chosen for contact interaction between diaphragm and all pump components including self-contact. As for all contact interaction with fluids, a rough friction was chosen to model the no slip condition between fluids and solids.

3.3.6 Solver

The solver information that was used in this study is as follows.

- Solver = Abaqus/Explicit 2017 double precision
- CPU = Intel® Xeon® E5-2667 v2 at 3.3GHz
- Number of cores = 16
- Operating system = Red Hat Enterprise Linux Server

CHAPTER 4: RESULT & DISCUSSION

4.1 Introduction

In this chapter, results from Coupled Eulerian-Lagrangian and fully Lagrangian domain are shown. In CEL analyses, results from various pump speed and fluid viscosities are shown to evaluate its sensitivity to those parameters. These results are then compared with fully Lagrangian domain with fixed pressure surfaces of compressed air. Finer diaphragm meshes of fully Lagrangian domain were also shown to observe the sensitivity of mesh densities.

4.2 CEL - Sensitivity to Pump Speed

Figure 4.2 shows the maximum principal nominal strain output for pump speed of 100, 350 & 600 cycles per minute (cpm). Other than that, from the same figure we can also observe the fluid flow inside the chamber and the deformation of the diaphragm.

The highest magnitude of the nominal strain remains below 30% at various pump speed. The CEL analyses predict that the lower the pump speed, the higher the nominal strain of the deformed diaphragm. This might be because of reduction of momentum in diaphragm as a result of slower pump speed. We can also observe that the deformation of the diaphragm is consistent for various pump speed. However, at the highest pump speed of 600 cpm, the highest nominal strain is predicted to shift to the center of the diaphragm which is near the clamping disc. This could be because of the high speed of the shaft moving upwards, causing higher strain in that region as it need to push fluids away faster. In other words, the center area experience higher forces from the fluids due to high pump speed.

The local buckling of the diaphragm that was induced by fluid flow can be seen from the CEL analyses. However, due to low nominal strain, it shouldn't be a problem to operate at high cycle or with high fatigue life. Due to absent of fatigue test data, we are not able to predict the fatigue life of the diaphragm. However, since the break strain of this particular FKM material is around 300%, which is considerably higher than these results, it is reasonably safe to assume that this diaphragm design will not have problem in high cyclic applications.

The summary of computational time, highest magnitude of nominal strain and the ratio of kinetic to internal energy are shown in Table 4.1. As expected, the higher pump speed will result in smaller analysis step time, hence the Abaqus/Explicit solver requires less computational time. The relation between computational time and pump speed is shown in Figure 4.2. The computational time can be seen started to flatten out after 350cpm pump speed. The ratio of kinetic to internal energy remains less than 10% throughout the analysis for all of the cases. This means that the diaphragm deforming in a quasi-static manner through the pump stroke.

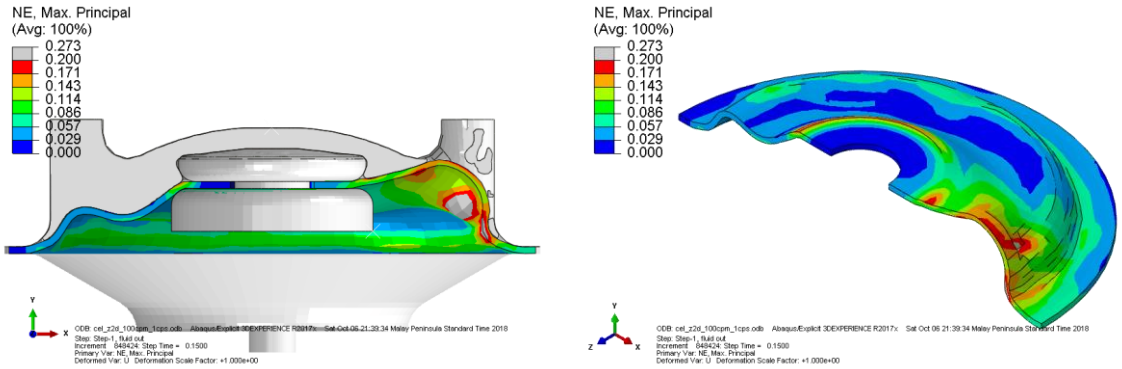

100 cycles per minute

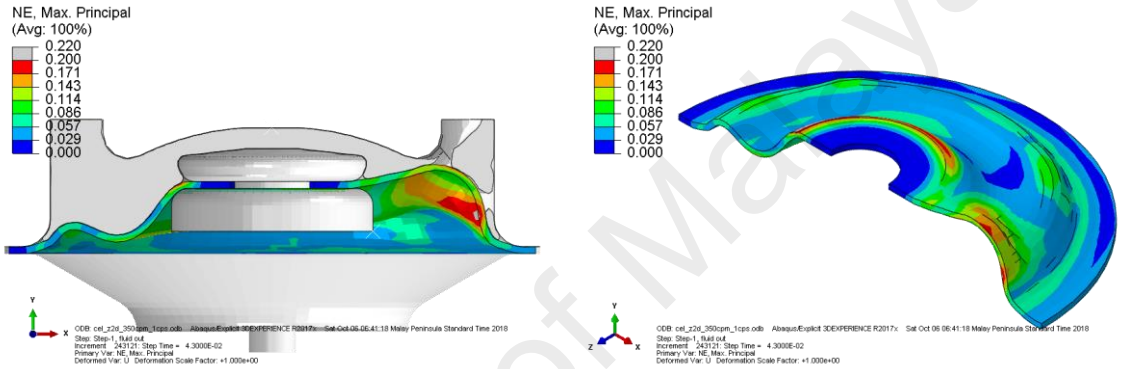

350 cycles per minute

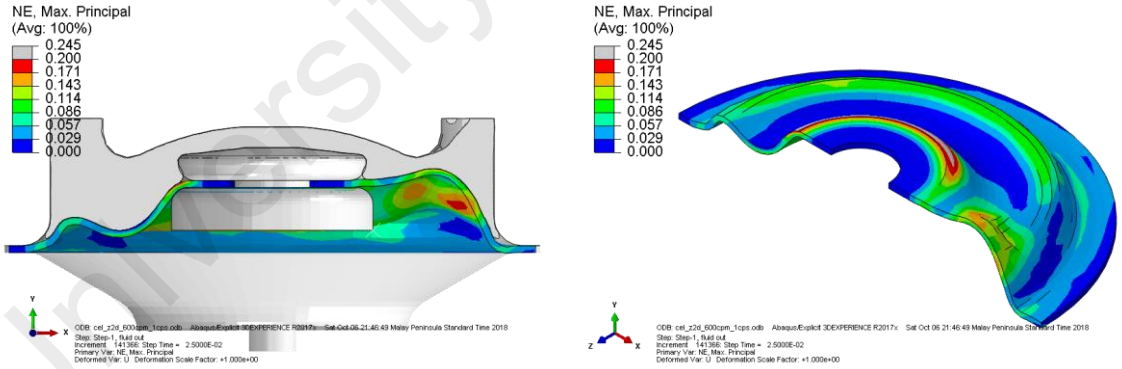

600 cycles per minute

Figure 4.1: Contour plot of maximum principal nominal strain (tensile) for different pump speed using 1mPa.s shear viscosity.

Table 4.1: Comparison between CEL analyses with different pump speed using 1mPa.s shear viscosity

Pump Speed (cpm)	Computational time (hh:min:sec)	Maximum Principal Nominal Strain (Tensile) (%)	Ratio of kinetic to internal energy at the end of step (%)
100	21:53:38	27.3	0.5
350	06:38:57	22.0	1.7
600	04:03:56	24.5	7.0

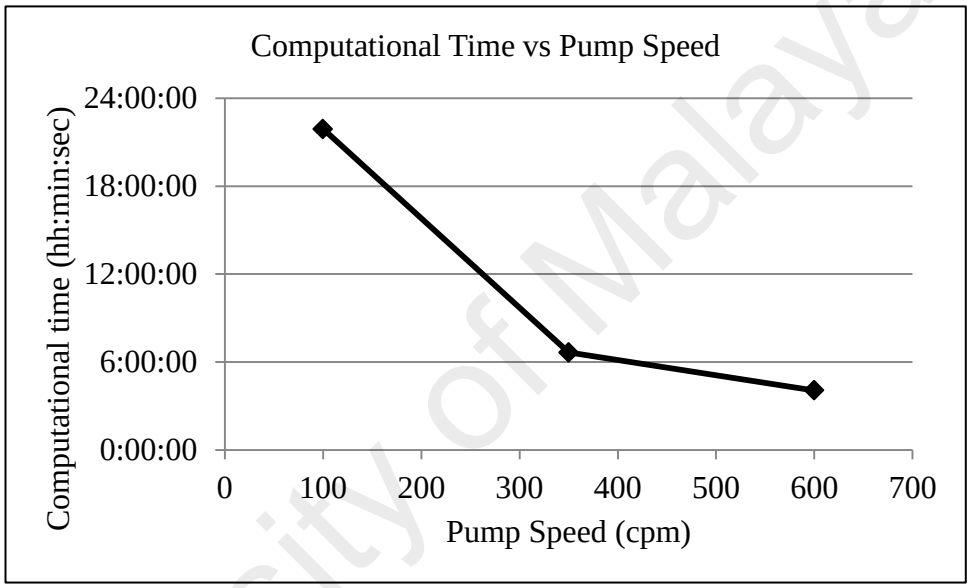

Figure 4.2: Relationship between computational time and pump speed.

4.3 CEL – Sensitivity to Fluid Viscosity

Figure 4.3 and Figure 4.4 shows the maximum principal nominal strain output for various fluid shear viscosities (1mPa.s, 10 mPa.s, 100 mPa.s, 1000 mPa.s, 10,000 mPa.s & 100,000 mPa.s) running at a constant pump speed of 350 cycles per minute. Other than that, in those figures we can also observe the fluid flow inside the chamber and also the deformation of the diaphragm. Note that 350cpm pump cycle was chosen for this sensitivity studies because it is within the chosen pump specification (max 400cpm) and it consistently shows stability with reasonable computational time.

The highest magnitude of the nominal strain remains below 30% when fluid viscosity is less than 10,000 mPa.s and peaks at 39% with fluid viscosity of 100,000 mPa.s. The results shows that as the fluid viscosity increases, the resistance to flow has increase and therefore higher forces are acting on the diaphragm due to higher fluid resistance to flow. As the result of that, the higher nominal strain observe on the diaphragm are as expected. Interesting to note that the CEL analysis predict that the location of highest nominal strain has move from near the pump outlet to the center of the diaphragm as the fluid viscosity increases. This can potentially help engineer to evaluate potential area of the diaphragm that will crack due to fatigue. The diaphragm deformation and strains from CEL analyses are found to be influenced by the fluid shear viscosity. This contradicts with the finding by van Rijswick (2017) using 3D shell diaphragm with FSI analysis. However, the difference could be due to different in designs of pump and diaphragm.

Similar to result from Chapter 4.2 above, the local buckling of the diaphragms that were induced by fluid flow can be seen from the CEL analyses. Also, as the highest nominal strain is about 13% of the material break strain, it is therefore reasonably safe to assume that it will not be a problem for high cyclic applications.

The summary of computational time, highest magnitude of nominal strain and the ratio of kinetic to internal energy are shown in Table 4.2. The computational time between various fluids viscosities remain fairly consistent around 7 to 8 hours except for analysis with 10 mPa.s which show some instability. The ratio of kinetic to internal energy remains less than 2% throughout the analysis which indicate that the diaphragm deforming in a quasi-static manner.

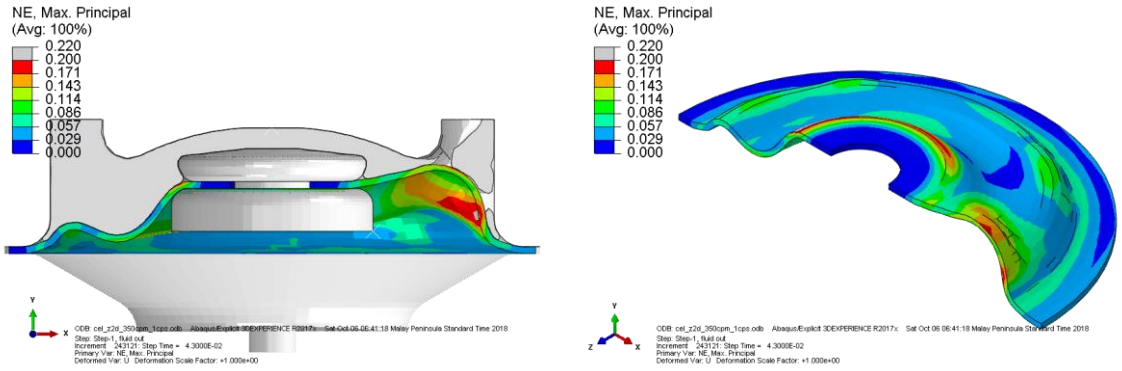

1mPa.s shear viscosity at 350cpm pump speed

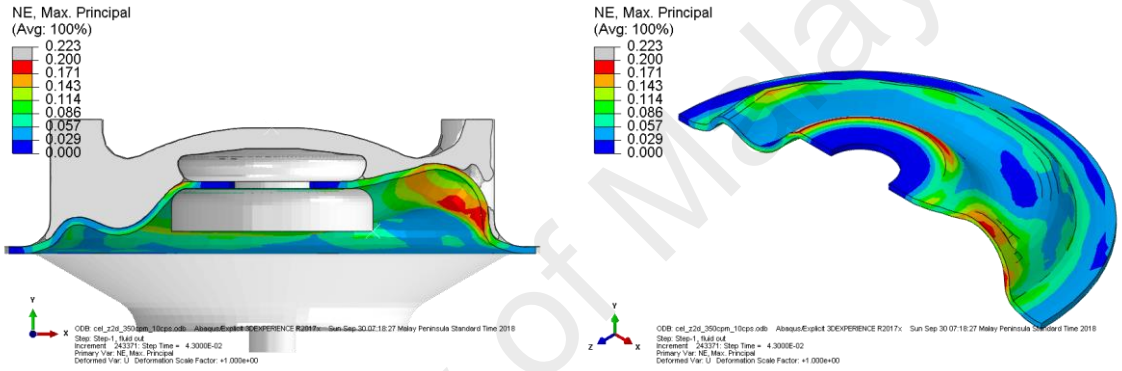

10mPa.s shear viscosity at 350cpm pump speed

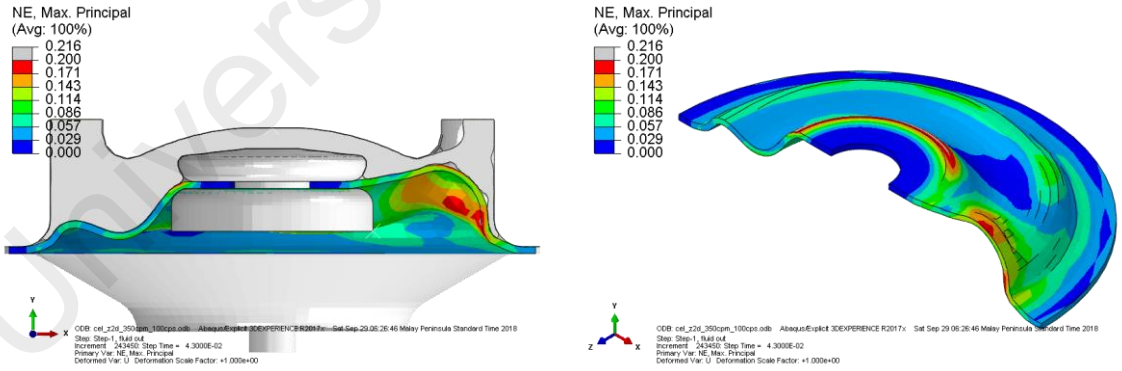

100mPa.s shear viscosity at 350cpm pump speed

Figure 4.3: Contour plot of maximum principal nominal strain (tensile) for 1mPa.s, 10mPa.s & 100mPa.s shear viscosity at 350cpm pump speed

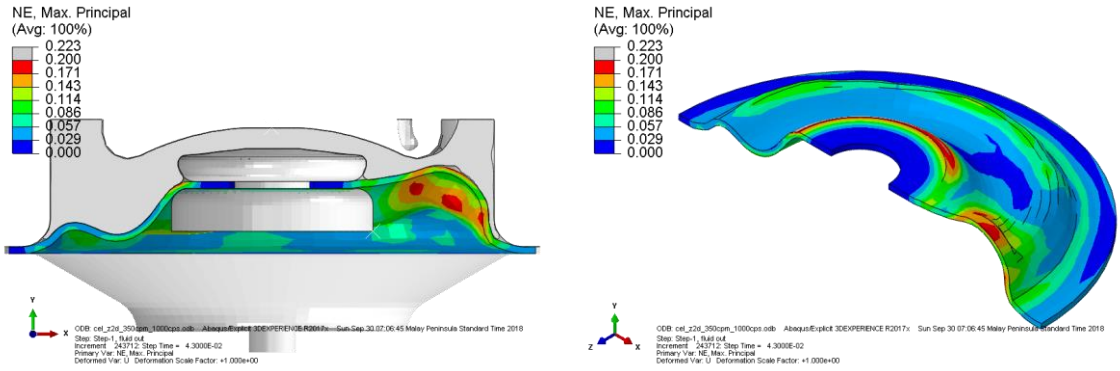

1,000mPa.s shear viscosity at 350cpm pump speed

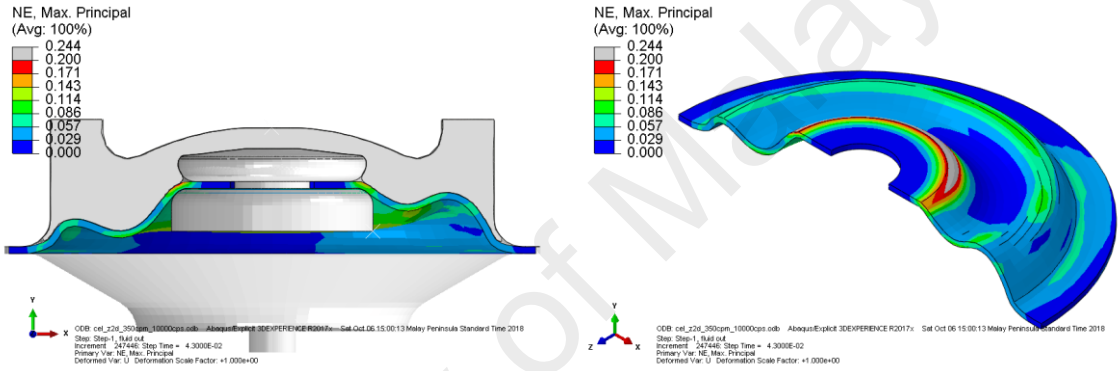

10,000mPa.s shear viscosity at 350cpm pump speed

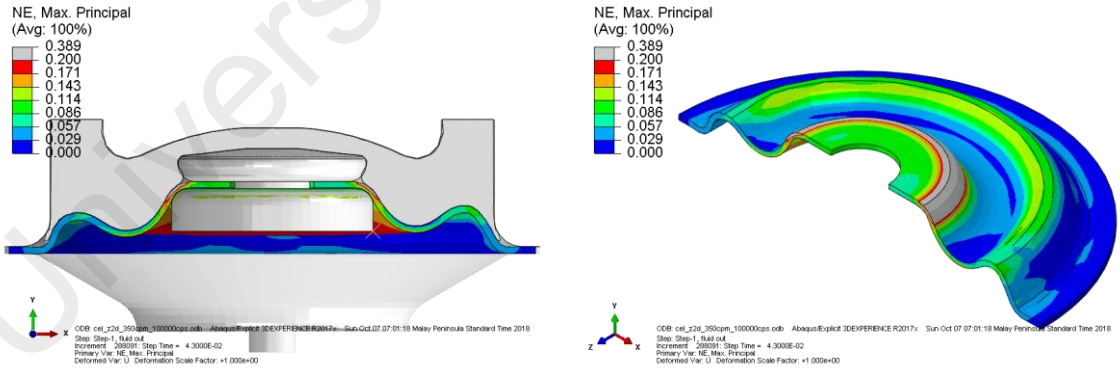

100,000mPa.s shear viscosity at 350cpm pump speed

Figure 4.4: Contour plot of maximum principal nominal strain (tensile) for 1000mPa.s, 10,000mPa.s & 100,000mPa.s shear viscosity at 350cpm pump speed

Table 4.2 Comparison of CEL analysis with 1mPa.s, 10mPa.s, 100mPa.s, 1000mPa.s, 10,000mPa.s & 100,000mPa.s shear viscosity at 350cpm pump speed

Fluid Viscosity (mPa.s)	Computational time (hh:min:sec)	Maximum Principal Nominal Strain (Tensile) (%)	Ratio of kinetic to internal energy at the end of step (%)
1	06:38:57	22.0	1.7
10	09:28:27	22.3	0.7
100	07:48:19	21.6	0.8
1000	06:50:18	22.3	0.9
10,000	06:40:11	24.4	0.7
100,000	07:30:19	38.9	0.1

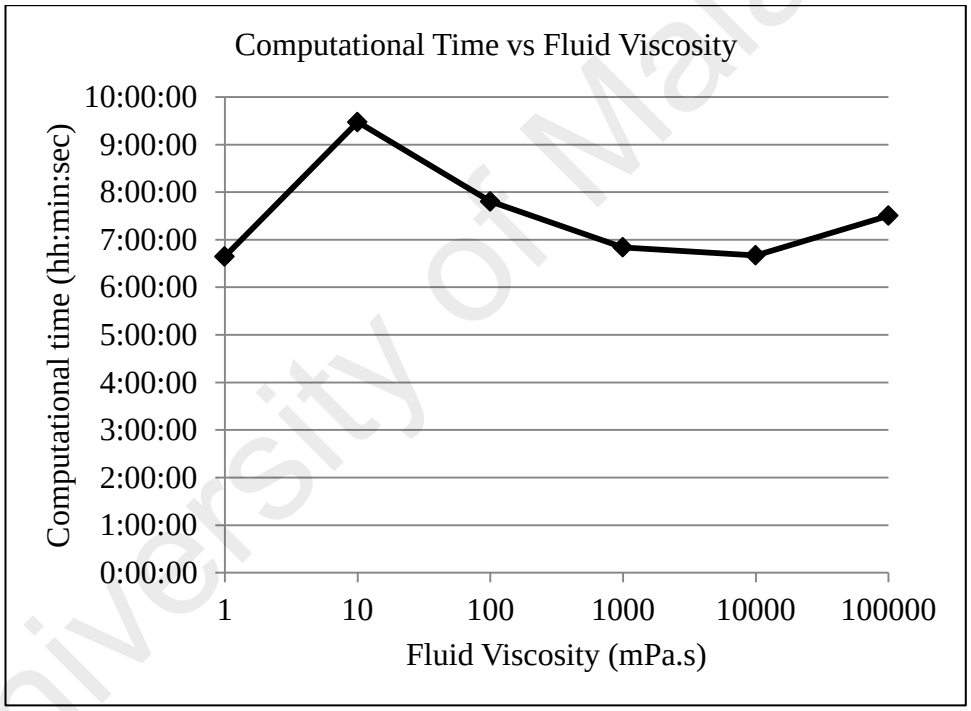

Figure 4.5: Relationship between computational time and fluid viscosity

4.4 Fully Lagrangian

Results from dynamic explicit FE analysis of fully Lagrangian domain using pressure difference of 0.005MPa on fixed pressure surfaces are shown in Figure 4.6 and Figure 4.7. The different between both models are the mesh density of the diaphragm as describe in Chapter 3.3.4 above. Briefly, the first model has the same mesh density as the CEL analysis and the second model has finer mesh along the circumference of the diaphragm.

The highest magnitude of the nominal strain remains below 20% for both models throughout the analysis. The posted result in Figure 4.6 and Figure 4.7 are the highest nominal strain during the pumping stroke. Similar to CEL analysis, there should be no concern of fatigue crack because of low nominal strain magnitude. However, with the absent of fluid induced deformation, the location of highest strain is at the convolute of the diaphragm.

The computational time has increase 6 fold between finer and coarse mesh as shown in Table 4.3. The increase in computational time is expected due to increase in number of degree of freedom (DOF). However, even with finer meshes, the computational time is considerably faster than the CEL analysis. The same table also shows that the ratio of kinetic to internal energy is very low (almost zero) which indicate that the diaphragm deforming in a quasi-static manner. However, the ratio was taken at the end of the analysis step and spike of kinetic energies can be seen especially during stroke reversal.

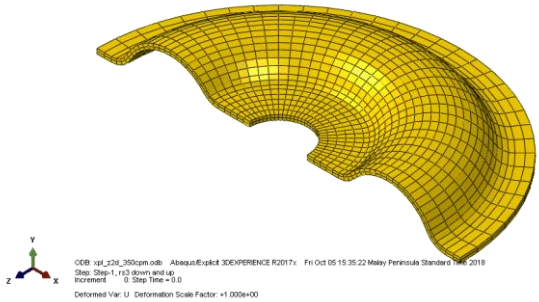

(a)

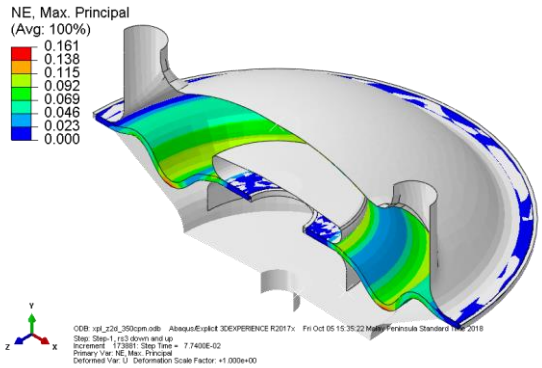

(b)

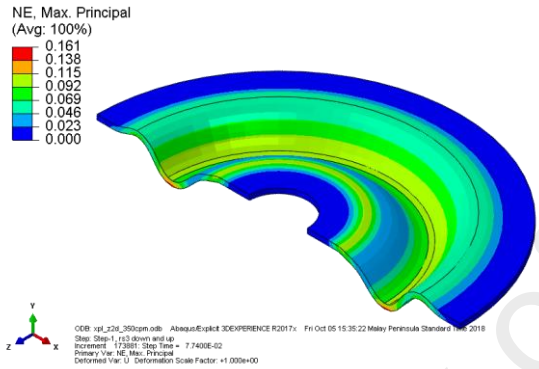

(c)

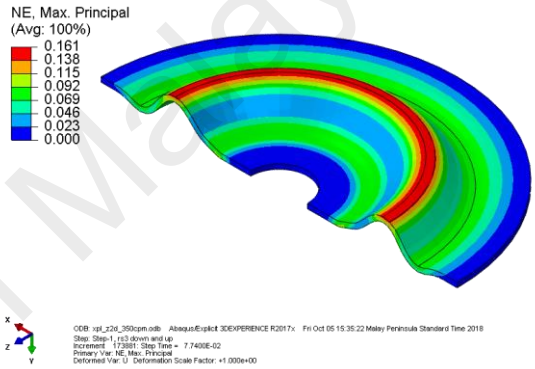

(d)

Figure 4.6: (a) Meshes on the diaphragm that is similar to CEL model; (b) to (d) Contour plot of maximum principal nominal strain (tensile) for fully Lagrangian model (shown in different views)

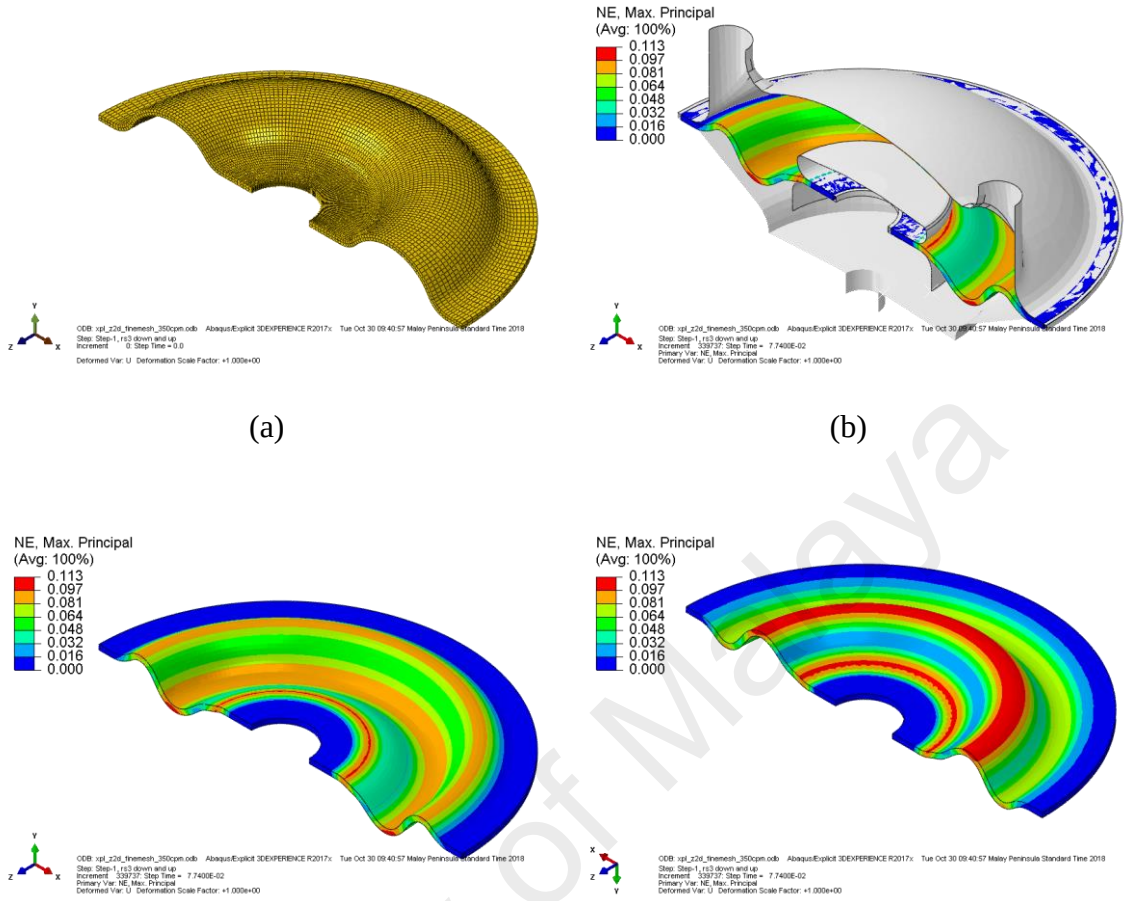

Figure 4.7: (a) Meshes on the diaphragm (fine mesh); (b) to (d) Contour plot of maximum principal nominal strain (tensile) for fully Lagrangian model (shown in different views)

Table 4.3: Comparison of fully Lagrangian analysis with coarse and fine meshes at 350cpm pump speed

Mesh description	Computational time (hh:min:sec)	Maximum Principal Nominal Strain (Tensile) (%)	Ratio of kinetic to internal energy at the end of step (%)
Coarse	00:05:40	16.1	0.04
Fine	00:31:41	11.3	0.03

4.5 Comparison between CEL and fully Lagrangian

The stable time increment for all CEL analyses is around $1.4x10^{-7}$ to $1.8x10^{-7}$ second. All CEL analyses were able to maintain a consistent stable time increment because of no local buckling (except induced by fluid flow), folding or highly distorted elements. Note that various simplifications that were done to the model help eliminate the possibility of local buckling, diaphragm folding and distorted elements. However, these simplifications were most likely to have some level of influence to the solution accuracy but are unavoidable due to limited resources in this study.

As for fully Lagrangian analyses, the stable time increment is $2.3x10^{-7}$ and $4.6x10^{-7}$ second for fine and coarse mesh respectively. As results shown above, the higher stable time result in faster computational time. However, the fully Lagrangian analysis were not able to capture the fluid induce deformation or any local buckling during change of stroke (from fluid suction and discharge). Without actual testing, it is not possible to know whether the absent of local buckling is due to the limitation of FE codes or if it is the actual deformation of the diaphragm.

Instability is observed in the CEL model whenever snap-through or local buckling is about to occur. The posted results didn't show these instability as the posted simulations were perform from middle of stroke which is the 'as molded' shape of the diaphragm and a coarse mesh was applied to the diaphragm and fluids due to limited resources. On the other hand, the fully Lagrangian model was very stable and quick in terms of pre-processing and also computational time.

Kinetic energy remains low in CEL and purely Lagrangian models. With the kinetic energy less than 10% of internal energy, the analysis can still be considered as quasi-static (LeDuc Jr. & Yeoh, 2006). Therefore, there is some room for improving the computational time.

CHAPTER 5: CONCLUSIONS & RECOMMENDATION

5.1 Conclusion

In this study, an elastomeric diaphragm concept has been developed. It is based upon commercially available air operated double diaphragm (AODD) pump with some defeaturing or simplification to aid in convergence of the FE analysis.

The CEL analysis is found to be able to induce diaphragm deformation due to fluid flow of the membrane pump. However, it is unstable and requires very long computational time. Lots of compromise or model simplification need to be made to obtain the convergence. Some of the simplification could affect the accuracy of the analysis. The deformation and nominal strain on the diaphragm remain generally consistent with various pump speed and fluid viscosities in CEL analyses.

On the other hand, the fully Lagrangian analysis is very stable but will not able to simulate the deformation due to fluid flow. Both types of analyses are found to not able to capture the snap-through behavior of the diaphragm. However, it is unknown if the actual diaphragm exhibit such behavior.

5.2 Recommendation

In future, it is recommended to study the effect of simulation a 360° model instead of 180°. This allows the diaphragm to develop any local buckling or folding pattern without the influence of symmetric boundary condition. The initial attempt with 360° model in CEL was unsuccessful due to large number of meshes or degree of freedom to be calculated. Due to limited resources, a compromised was made with 180° model and coarser meshes.

On top of that, the FE analysis can be run with parameters as specifies by the pump manufacturer and actual test should be done to correlate the FE result. In this study, low compressed air pressure was use (14.5psi) instead of 30psi to 100psi as specified by the manufacturer.

Finally, a 3D diaphragm model with hydrostatic pressure or a two-way FSI co-simulation with CFD codes coupled with FEA structural codes should be considered for a possible tool for evaluating this problem. The analysis should be for more than one full cycle to observe the snap-through during the change of pressure from discharge and suction.

REFERENCES

Optimised diaphragm design. (2004). *World Pumps, 2004*(457), p. 7. doi:https://doi.org/10.1016/S0262-1762(04)00344-X

Aerts, R., & Gut, M. (2007). Ceramics and diaphragm pumps – a good match? *World Pumps, 2007*(495), pp. 34-36. doi:https://doi.org/10.1016/S0262-1762(08)70067-1

Alberto, M. B., Manuel, F. O., & Andrés, M.-F. (2019). Numerical methodology for the CFD simulation of diaphragm volumetric pumps. *International Journal of Mechanical Sciences, 150*, 322-336. doi:https://doi.org/10.1016/j.ijmecsci.2018.10.039

Ali, A., Hosseini, M., & Sahari, B. B. (2010). A Review of Constitutive Models for Rubber-Like Materialas. *American J. of Engineering and Applied Sciences*, 3 (1): 232-239.

Bakroon, M., Daryaei, R., Aubram, D., & Rackwitz, F. (2017). Arbitrary Lagrangian-Eulerian Finite Element Formulations Applied to Geotechnical Problems. *Workshop on Numerical Methods in Geotechnics.* Hamburg, Germany.

Blades, E. L., Luke, E. A., Kurkchubashe, A. G., Collins, E. M., & Miskovish, S. R. (2010). A Fluid-Structure Interaction Simulation Capability Using the Co-Simulation Engine. *SIMULIA Customer Conference.* Providence, Rhode Island: Dassault Systèmes Simulia Corp.

Bowan, G. J. (1997). Specifying air-operated double-diaphragm pumps. *World Pumps, 1997*(364), pp. 38-39. doi:https://doi.org/10.1016/S0262-1762(97)86578-9

Brinson, H. F., & Brinson, C. L. (2015). *Polymer engineering science and viscoelasticity: An introduction.* Evanston: Springer Verlag.

Brito, E., & Jack, R. (13 de Nov de 2016). AODD Pumps in Chemical Processes. *Chemical Week Assoc*, p. 8.

Bubb, A., & Freissler, B. (2010). Developments in metering diaphragms. *World Pumps, 2010*(5), pp. 24-26. doi:https://doi.org/10.1016/S0262-1762(10)70090-0

Chmelnizkij, A., Nagula, S., & Grabe, J. (2017). Numerical simulation of deep vibration compaction in Abaqus/CEL and MPM. *1st International Conference on the Material Point Method* (pp. 302-309). Procedia Engineering 175.

Ducobu, F., Arrazola, P. J., Rivière-Lorphèvre, E., Ortiz de Zarate, G., Madariaga, A., & Filippi, E. (2017). The CEL method as an alternative to the current modelling approaches for Ti6Al4V orthogonal cutting simulation. *16th CIRP Conference on Modelling of Machining Operations* (pp. 245-250). Procedia CIRP 58.

Freudenberg Simrit GmbH & Co. KG. (2007). Technical Pinciples - Diaphragms. *Simrit Technical Manual*. Freudenberg Simrit GmbH & Co. KG.

Georgiadis, S. (1988). Beitrag zur Berechnung de Beanspruchung kreisrunder Metallmembranen (Doctoral dissertation). Universität Erlangen-Nürnberg.

Graco Inc. (10 de October de 2018). *Husky 515 Air-Operated Diaphragm Pumps*. Fonte: http://www.graco.com/gb/en/products/process/husky-515-double-diaphragm-pump.html

Jack, R. (2015). Considerations for diaphragm selection. *World Pumps, 2015*(1), pp. 30-32. doi:https://doi.org/10.1016/S0262-1762(14)70346-3

James, A. G., Green, A., & Simpson, G. M. (1975). Strain energy functions of rubber. I. Characterization of gum vulcanizates. *J. Appl. Polym. Sci., 19*, 2033-2058.

Johnson, M. A. (2014). Diaphragm technology with abrasive fluids. *World Pumps, 2014*(10), pp. 14-16. doi:https://doi.org/10.1016/S0262-1762(14)70236-6

LeDuc Jr., M. S. (28 de April de 2003). Strain vs. Stress - Discusson on using Strain vs. Stress for Posting Failure in Elastomeric Components. *FNGP FEA Newsletter Articles and Presentation*. Northfield, New Hampshire, United States of America.

LeDuc Jr., M. S., & Yeoh, O. H. (6 de Jan de 2006). *Demolding Simulation Using Finite Element Analysis: Current State of Technology and Future Direction.* Freudenberg-NOK Technical Report, Bristol, NH & Plymouth MI.

Li, F., Ding, P., & Sibal, S. (2010). Coupled Fluid / Structure Interaction Simulation Using Abaqus CEL. *SIMULIA Customer Conference.* Providence, Rhode Island: Dassault Systèmes Simulia Corp.

Mimmia, G., & Pennacchi, P. (2001). Diaphragm design improvement for a metering pump. *Engineering Failure Analysis 8 (2001) 1-13*.

Moaveni, S. (2015). *Finite Element Analysis, Theory and application with ANSYS.* Upper Saddle River, NJ: Pearson.

Nieminen, V. (2015). *Fluid-structure interaction simulation utilising MpCCI.* Finland: VTT Technical Research Centre of Finland.

Qiu, G., Henke, S., & Grabe, J. (2009). Applications of Coupled Eulerian-Lagrangian Method to Geotechnical Problems with Large Deformations. *SIMULIA Customer Conference.* Rhode Island: Dassault Systèmes Simulia Corp.

Rivlin, R. (1956). Chapter 10. In: F. Eirich, *Rheology: Theory and Applications.* New York: Academic Press.

Rozee, D. (2016). Cost benefits and energy efficiencies of AODD pumps. *World Pumps, 2016*(1), pp. 34-36. doi:https://doi.org/10.1016/S0262-1762(16)30033-5

Schlücker, E. (1993). Zur Optimierung kreisrunder Plastomermembranen für oszillierende Verdrängerpumpen (Doctoral dissertation). Universität Erlangen-Nürnberg.

Sillem, A. (2008). Feasibility study of a tire hydroplaning simulation in a finite elemetn code using coupled Eulerian-Lagrangian method (MSc Thesis). Delft university of technology.

Simulia. (2006). *Training module - Introduction to ABAQUS V6.6.* Dassault Systèmes Simulia Corp.

Simulia. (2015a). *Training Module - Abaqus/Explicit: Advance Topics V6.14.* Dassault Systèmes Simulia Corp.

Simulia. (2015b). *Training module - Modeling extreme deformation and fluid flow with Abaqus V6.14.* Dassault Systèmes Simulia Corp.

Simulia. (2016). Abaqus 2016 Documentation. Dassault Systèmes Simulia Corp.

Söderholm, C. (2008). The future of air operated double diaphragm pumps. *World Pumps, 2008*(502), pp. 22-23. doi:https://doi.org/10.1016/S0262-1762(08)70205-0

Stahl, W. M. (2006). Choosing the right elastomer for the right application. *World Pumps, 2006*(481), pp. 30-33. doi:https://doi.org/10.1016/S0262-1762(06)71110-5

Standard Pump, Inc. (2013). *Sanitary Air Operated Diaphragm Pumps.* Fonte: https://www.rodem.com/sites/default/files/literature/AODD-Sanitary-Standard-pump.pdf

van Rijswick, R. (2017). Fluid structure interaction in piston diaphragm pumps (Doctoral dissertation). Delft University of Technology. DOI: 10.4233/uuid:2f24e261-003f-4e80-ba4e-0b0c1caecdf7.

Völkl, L. (1992). Einspanneffekte an Membranen von Membanpumpen und -verdichtern (Doctoral dissertation). Universität Erlangen-Nürnberg.

Warren, P., & Smith, P. (2007). Selection guide – considerations for elastomer diaphragms. *World Pumps*(2007), pp. 36-38. doi:https://doi.org/10.1016/S0262-1762(07)70035-4

Wilden Pump & Engineering, LLC. (2018). AODD pumps for chemical processes. *World Pumps, 2018*(7), pp. 28-30.

Xiaoying, S., Jian, M., & Chunlong, Z. (2016). Fluid-Structure Interaction Analysis Using Finite Element Methods for IRWST for Reactor Building. *International Youth Nuclear Congress*, 225-233.

Yeoh, O. H. (1990). Characterization of Elastic Properties of Carbon-Black-Filled Rubber Vulcanizates. *Rubber Chemistry and Technology, vol 63-5,* 792-805.